ORIGINAL PAPER

Morphological experimental study of bone stress at the interface acetabular bone/prosthetic cup in the bipolar hip prosthesis

D. ANUŞCA[1)], I. E. PLEŞEA[2)], N. ILIESCU[4)], P. TOMESCU[3)], F. POENARU[1)], V. DASCĂLU[1)], O. T. POP[2)]

[1)]*Department of Orthopedics*
[2)]*Department of Pathology*
[3)]*Department of Urology*
University of Medicine and Pharmacy of Craiova
[4)]*Department of Material Resistance,*
Polytechnics University, Bucharest

Abstract

By calculating the tension and distortion of the elements composing the bipolar prosthesis under extreme conditions encountered in real life using a special post-processing program, we established the variation curves of the contact pressure at the hip bone-cup, armor-cup and cup-femoral head interface. By comparing the data obtained from all the examined cases, important conclusions were drawn regarding the influence of tension and pressure distribution on the structural integrity and biomechanics of the prosthesis, as well as the acetabular wear and tear, in order to assess its reliability. The experimentally determined tension and distortion status at the acetabular bone-metal armour interface, lead to the wear and tear phenomenon, which can be explained by three mechanisms and theories incompletely reflecting the overall process. The histopathologic study of the acetabular bone tissue using FEM (finite elements method) on surgically removed specimens will probably lead to the identification of a series of factors that could reduce the rate of the wear and tear process.

Keywords: acetabular bone, bipolar hip arthroplasty, finite elements method.

Introduction

The structure of acetabular bone is very important concerning the disposition and the orientation of the bone lesions, mainly the traumatic ones. The external zone consists of dense connective tissue. The articular surface is covered by a framework of fibrils beneath there is a layer of connective fibers with an orientation almost lamellar. The internal zone has a fibro-cartilaginous structure with predominance of collagen type II fibers with a circular orientation. The blood vessels come in the acetabular eyebrow from the adjacent particular capsule and they have an irregular distribution only to the peripheral third of eyebrow [1].

With ageing, degenerative changes will develop in the acetabular bone, especially on the acetabular eyebrow. One of the most important factors involved in this process is the pressional mechanic stress on the interface between the femoral head and acetabular bone, especially on the acetabular eyebrow [2, 3].

Femoral neck fracture is the most ill-fated fracture in the entire bone and articular traumatology. Although it is considered a revolutionary technique, hip arthroplasty did not solve the problem of acetabular and femoral wear and tear. The purpose of bipolar prothesis is the use of interior articular prostetics in order to reduce tension and the wear and tear phenomenon accompanied by loss of bone tissue in the acetabulum. In spite all these, at the bone-prothesis interface the wear and tear process eventually begins, requiring the replacement of the bipolar prothesis with a total hip prothesis. There are several theories and mechanisms that offer an incomplete explanation of the wear and tear phenomenon and its clinical repercussions.

The purpose of this study is to identify the areas of the acetabulum at the bone-prothesis interface with the highest stress by determining the deformation and the tensions inside a bipolar prothesis and the acetabulum using experimental models realised with the finite elements method. The identified stress areas using numerical investigations (modeling of the components of the hip hinge using FEM) could then be histopathologically studied in order to reveal possible factors that could influence wear and tear process.

Material and methods

The experimental study using the finite elements method implies decomposing the analyzed structures in octahedral units small enough to accurately approximate the 3D geometry and properties of the structures that are to be analyzed. The materials consisted of a BIOMET bipolar acetabular cup with an outer diameter of 48 mm, standard neck and a prosthetic head 28 mm in diameter, adequate for our available pelvis. Postero-anterior and lateral incidence radiographs of this joint were performed, illustrating two phases of the walking process (Figures 1 and 2).

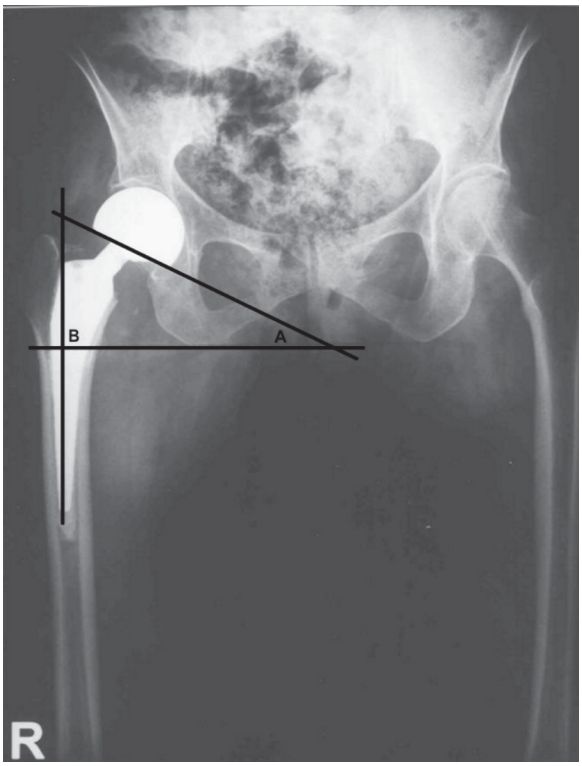

Picture (a) – ***Anterior-posterior view. The hip is in neutral position***

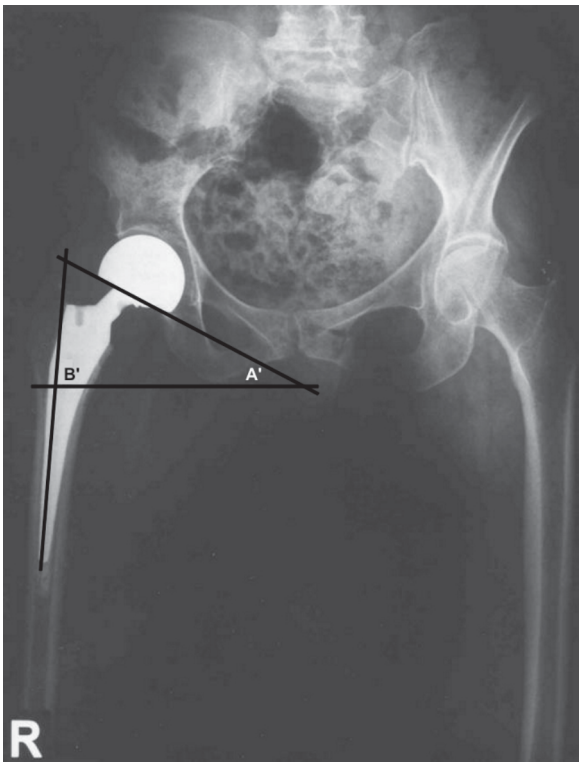

Picture (b) – ***Anterior-posterior view. The hip is in abduction***

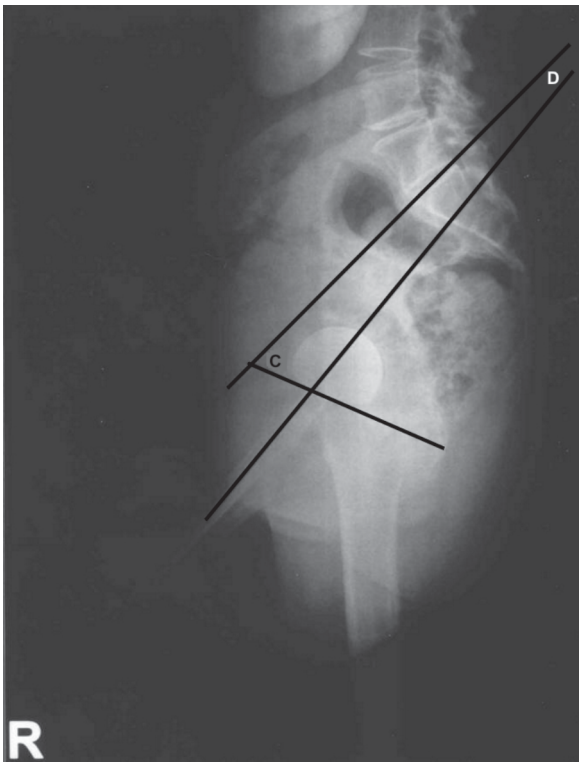

Picture (c) – ***Lateral view. The hip is in 10^0–15^0 extention, simulating the stepping***

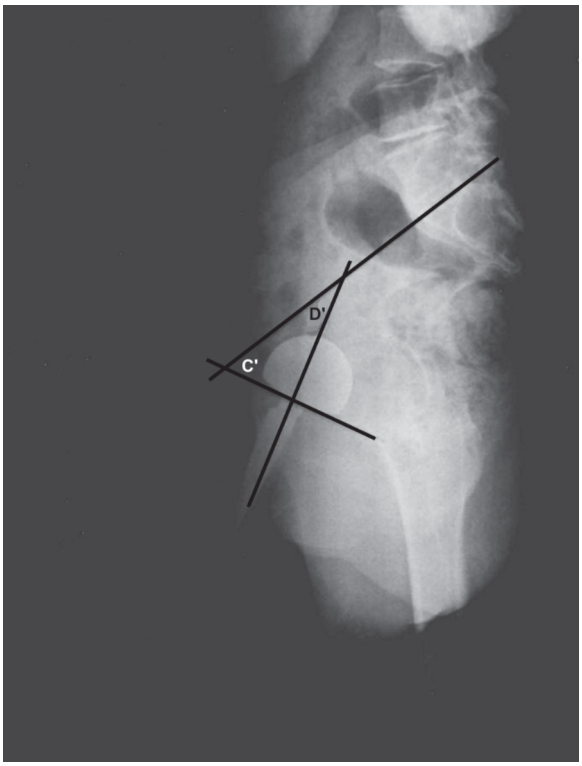

Picture (d) – ***Lateral view. The hip is 10^0–15^0 flexion, simulating the stepping***

Figure 1 – ***Pelvis X-rays in upright posture and monopod support***

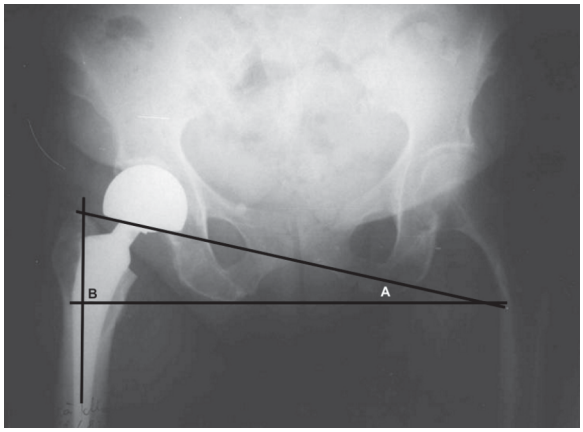

Picture (a) – ***Anterior-posterior view. The hip is in neutral position***

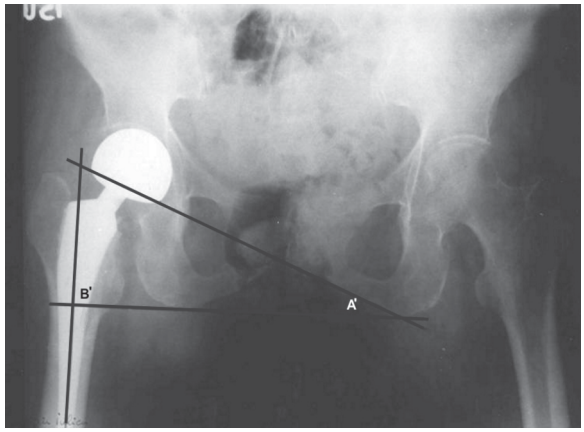

Picture (b) – ***Anterior-posterior view. The hip is in abduction***

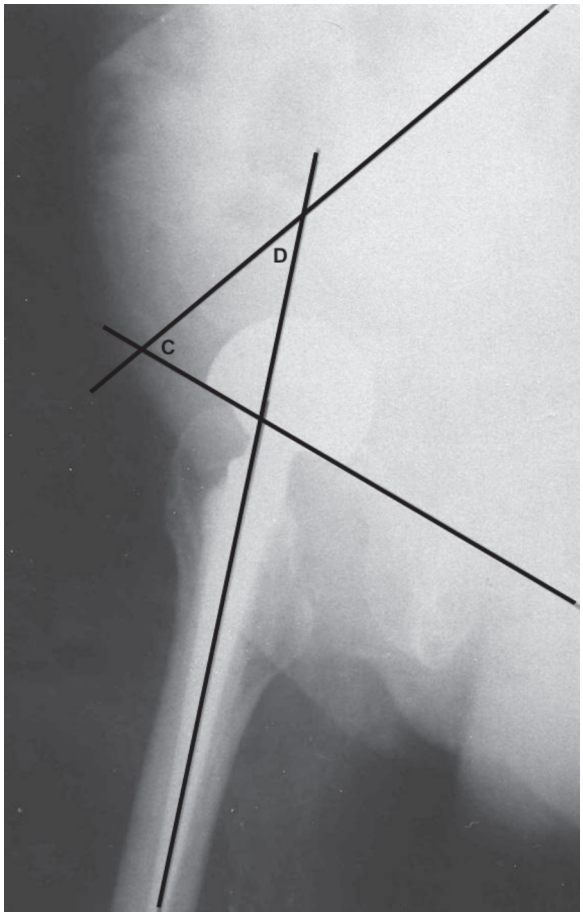

Picture (c) – ***Lateral view. The hip is in 10^0–15^0 extention, simulating the stepping***

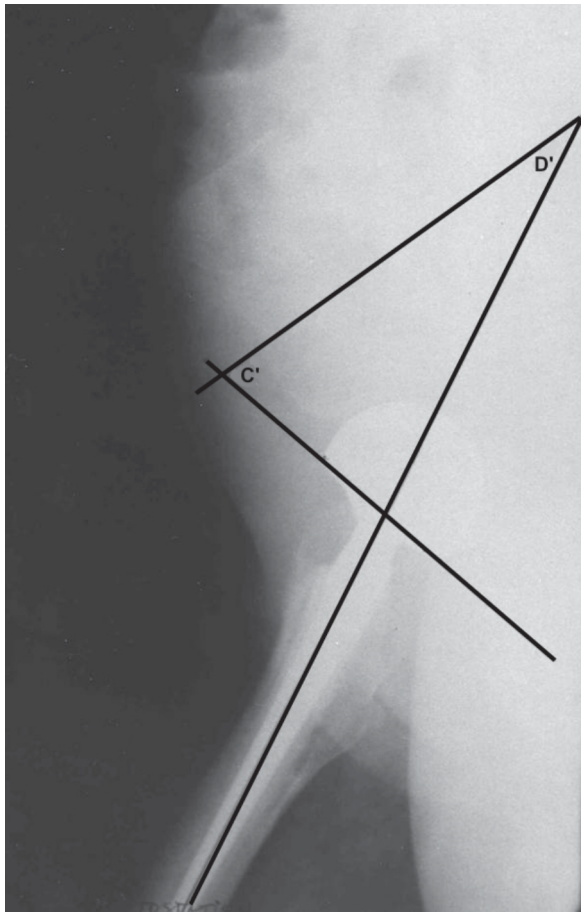

Picture (d) – ***Lateral view. The hip is 10^0–15^0 flexion, simulating the stepping***

Figure 2 – ***Pelvis X-rays in upright posture and bipodal support***

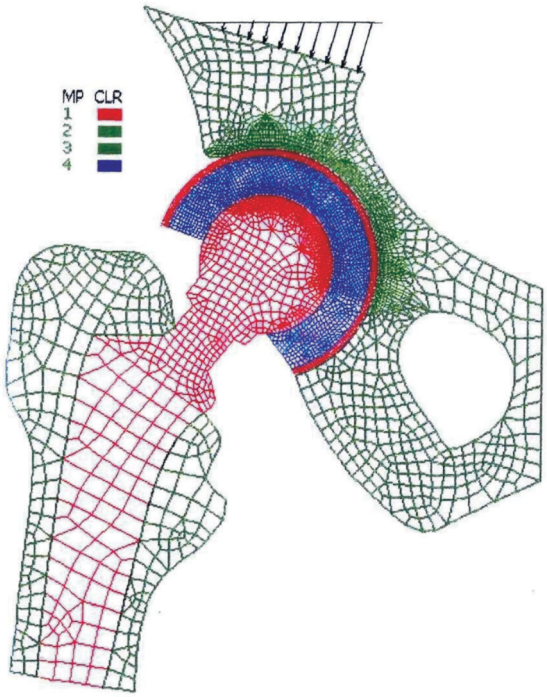

Picture (a) – ***Frontal section and monopod support***

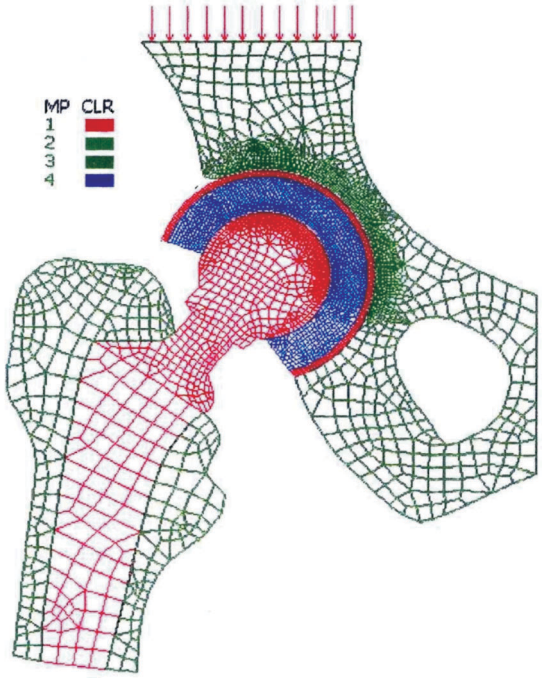

Picture (b) – ***Frontal section and bipedal support***

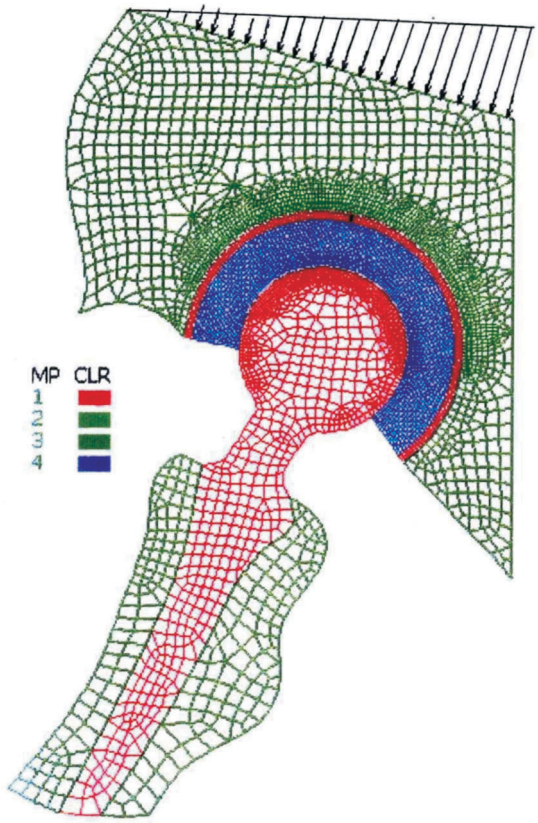

Picture (c) – ***Sagittal section and monopod support***

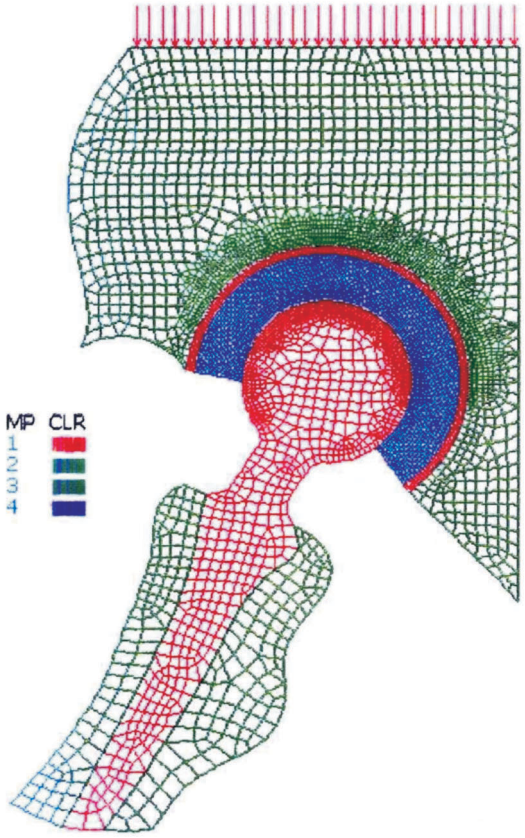

Picture (d) – ***Sagittal section and bipedal support***

Figure 3 – ***The analysis of the tension and deformation status in the four extreme conditions encountered in real life***

The extreme complexity of the calculus made the study of the bipolar cup behavior impossible. In the same time, serial axial CT scans (every 2 mm) of the same articular model were performed starting at 3 cm above the acetabular dome and finishing at 1 cm below the inferior acetabular end. The images obtained were scanned and then a sufficient number of points were marker on the outline and related to a 3D coordinate system (XYZ).

The 3D geometrical model was obtained by computer aided assembling of the points resulted from the radiographic composing and the CT scans and then it was discretised by adding a number of 30 000 points that served in obtaining the finite elements model.

In order to proceed, the prosthetic elements were modulated in two planes (frontal and sagital), with isoparametric elements with four knots with two degrees of freedom per knot and thus resulting a plane model, 8 mm thick.

Special "GAP"-type quadrilateral contact elements (L = 5 mm) were used to modulate the contacts. We considered that at the interface between the prosthetic components there is an initial space of 0.1 mm.

Contact modulation required the introduction of some special conditions on the outline that wouldn't affect the mechanical behavior of the overall analyzed model. Thus, we introduced two "SPRING"-type elastic elements for vertical translation, with negligible rigidity, placed in two knots at the upper extremity of the hipbone (Figure 3).

We also considered that the knots placed on the symphysis direction could move only vertically and that the inferior portion of the femoral body is embedded.

Biomechanical aspects

During the successive positions of the limbs while walking, the weight of the body is transmitted in different ways to the femoral bone through the hip, varying with their position and support way.

Thus, in the bipedal support, the weight of the body is equally distributed to the limbs. In the monopod support, encountered in most phases of the walking process, the weight force of the body (G) and the equilibrium force generated by the buttock muscles (F) are composed and the resulting force (R) (Figure 4) is acting upon the upper femoral extremity, in the frontal plane, at an angle of 16 degrees with the vertical through the center of the femoral head.

The action of this force produces a complex state of tension on the supportive cotyloid surface and inside the femoral bone tension that under certain extreme conditions determines femoral fractures at different levels or cartilage degeneration at the contact area between the cotyle and the femoral head [4–8].

If the hip joint is represented by a BIOMET bipolar hip prosthesis the action of the resultant force (R) is the same, producing a state of tension and deformation acting inside its structural components (armor, polyethylene cup, femoral head).

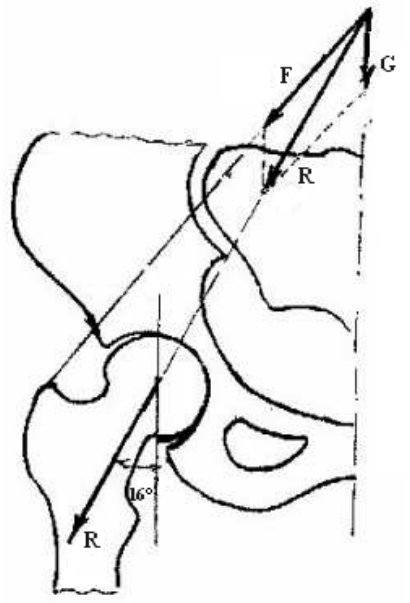

Figure 4

Considering a frontal section through the superior portion of a BIOMET bipolar hip prosthesis, the tension acting on a very small surface element (surrounding one point) situated for example in the polyethylene cup, is characterized by the tensions σ_x, σ_y and σ_{xy}, oriented according to an arbitrary xOy axis system (Figure 5).

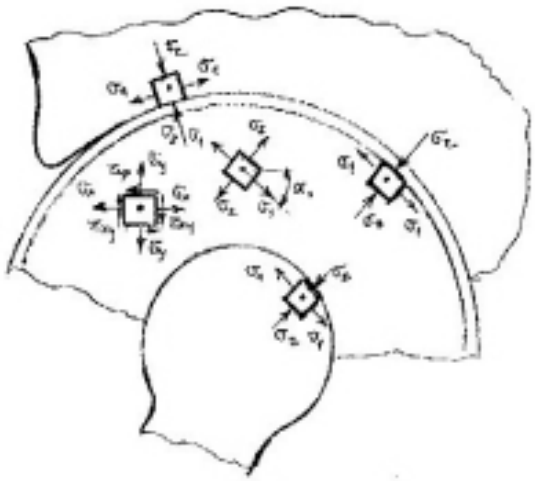

Figure 5

The tensions and their directions depend on the orientation of the surface element. Thus, for a certain orientation, the normal tensions a_x and b_y become in the same time the maximum and the minimum respectively, and the tangential tensions are null.

These tensions are the ***main tensions*** and are assigned σ_1 (the maximum value) and σ_2 (the minimum value), their directions being the ***main directions***, at an angle α_1 with the initial axes.

The main tensions and directions vary from one point to another of each structural component of the prosthesis and can be determined either by calculus using different methods such as (FEM), as well as experimentally, by using several investigation techniques such as the photoelasticity technique.

The state of tension developed in the proximity of the hipbone-armor interface, armor-cup interface and

cup-femoral head interface is characterized by a maximum compression tension σ_2 (absolute value) and a minimum stretch tension σ_1. The compression tension σ_2 is oriented along the normal direction to the contact surface and the stretch tension σ_1 is oriented along the tangent to this surface.

At the contact surface of the structural components of the prosthesis σ_2 is actually the contact pressure in that point (Figure 5) and σ_1 (small mad positive) can be used for calculating the rubbing forces acting on the contact surface [9–11].

The variation curve for the pressure on the contact surface can be obtained by determining the values for the main tensions σ_2 in different points in the proximity of the contact surface.

The distribution curve for the pressure shows a series of peaks (corresponding to very high pressure) depending on the contact between the two structural components.

While walking, between the structural components of the prosthesis there are only a few contact areas that change according to the position of the limbs. Thus, the pressure in each point of the contact area differs from one position to another.

The time related variation of this pressure respects a certain law called ***stress cycle*** (Figure 6a). The time necessary for a certain pressure value to repeat itself is called a **period** (T). Its reversed measure is called frequency and represents the number of periods repeated per time unit. The values are expressed in Hz (Hertz) [9, 10].

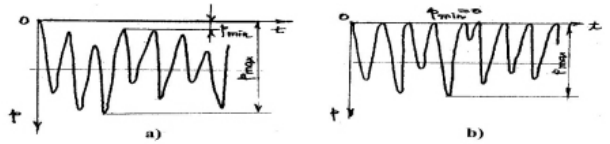

Figure 6

During the walking process the number of stress cycles is very high and the material in the contact area is submitted to the so-called contact stress phenomenon. In time, because of this contact stress, certain areas of the contact surface undergo a degenerative process, the most important being the plastification of the material. Thus, very high pressure values accumulate in certain micro structural discontinuity areas inside the material (at molecular or crystal level) that, in time, will lead to material failure and micro crack compensating mechanism is activation. These micro cracks develop towards the surface determining major changes of the contact geometry by crating plane or sunk areas.

Following these local changes, the contact between the components of the prosthesis during the walking process is discontinuous, under the form of beats, the material undergoing a ***negative stress pulse cycle*** [7, 8].

Aside from the destructions produced by mechanical factors, in certain areas of the structural components of the prosthesis one must take into consideration the changes that can be produced by certain biological factors. Thus, following the diffusion of certain particles from the prosthetic material into the bone tissue, the histiocyte formation and growth is triggered, leading to the so-called bone tissue retraction around the prosthesis and its aseptic loss.

The simultaneous degrading action of these biomechanical factors in time leads to the shortening of the prosthesis life period, and its earlier replacement.

In order to outline the local changes determined by the action of the mechanical factors in different areas of the BIOMET bipolar hip prosthesis along with the changes of the limb position and charge, we analyzed the tension and deformation status of its components using the finite elements method.

We calculated the tension and deformation of the prosthetic components in four extreme conditions encountered in real life (Figure 3, a, b, c and d):

1. Frontal section and monopod support;
2. Frontal section and bipedal support;
3. Sagital section, 15^0 flexion and monopod support;
4. Sagital section, 15^0 flexion and bipedal support.

We evaluated the tensional and deformational status in the planes taken into consideration for all the components of the prosthesis in all the cases.

Using all the data and a special post-processing program we traced the variation curves for the contact pressure at the components interface (hipbone-armor, armor-cup and cup-femoral head). We compared the post-processing data and draw a few important conclusions regarding the effect of the tensional status and contact pressure distribution on the structural integrity of the prosthesis and its biomechanical behavior, in order to establish its true reliability.

Model loading

The mathematical analysis was made for both monopod and bipedal support. For the monopod support we admitted that the center of the femoral head is under the action of a concentrated load (R) forming an angle of 16° with the vertical. This load is the resultant force of the body weight and the effort developed by the extension of the hip muscles (Figure 7).

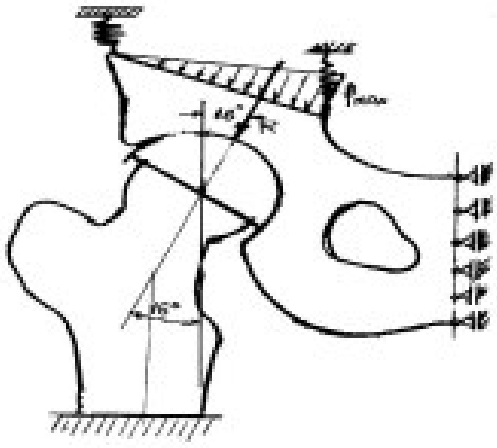

Figure 7

Admitting that the body weight (excepting the weight of the limbs) is G = 800 N and taking into the consideration several statements from the literature [1, 2, 4] that suggest that in monopod support R = 3G, we postulated that:

$$R = 3G = 3 \times 800\ N = 2400\ N = 2.4\ kN$$

In monopod support modeling, this load was obtained by applying a linearly distributed load in the knots of a linear contour of the upper portion of the hipbone (Figure 7).

The maximum linearly distributed load (p_{max}) and the distribution length were chosen so that we could obtain a resultant force R = 2.4 kN that would pass through the center of the femoral head at an angle of 16° with the vertical (Figure 7 and Figure 3, a and c).

In bipedal support modeling the body weight G = 800 N was equally distributed to the limbs and was transmitted to the femoral head under the form of an equally distributed load on a linear contour of the upper portion of the hipbone (Figure 3, b and d).

Calculus of the tensional and deformational status using FEM

In order to calculate the tensional and deformational status using FEM, the models for the analyzed structures obtained by knot linked quadrilateral finite elements discreeting, were loaded as mentioned above. In the same time we introduced the above-mentioned contour restrictions by reducing the number of degrees of freedom of some knots (the ones from the symphisis), in agreement with the reality.

We used the equation of the finite elements method, written as a matrix especially for the particular case of a tension and deformation field under static conditions, for each model:

$$[K]\{u\}=\{F\}$$

where [K] is the rigidity matrix, {u} is the column vector for the displacement and {F} is the column vector for the exterior forces [10, 14–16].

Knowing all the constants that characterize the material of the prosthesis we can calculate the displacement of the knots by solving the equation system obtained after using the equation of the finite elements method.

Depending on the components of the displacement vectors we can express the specific deformation for each point of the structural model that is analyzed using the linkage matrix interpolation functions.

We can finally calculate the tension for each point of the model by using Hooke's generalized law and the elasticity matrix of the material. Depending on the available post-processing programs, the results can be eloquently expressed on charts in which the areas of constant tension are represented using a code of colors.

The elastic characteristics of the materials used in our models are presented in Table 1.

Table 1

Material	Elasticity Module E [MPa]	Transverse contraction coefficient u
Steel	2.10×10^5	0.30
Femoral bone	1.41×10^4	0.23
Hip bone	1.65×10^4	0.24
High density polyethylene	1.25×10^3	0.27

The calculus characteristics for the analyzed models (number of knots, number of elements, number of equations and number of contact elements) are shown in Table 2.

Table 2

Condition no.	No. of knots	No. of elements	No. of contact elements	No. of equations	The distribution force applied to the model [MPa]
1	5733	5531	202	11470	$f_{max} = 12.77$
2	5663	5466	202	11330	f = 0.833
4	6655	6450	222	13270	$f_{max} = 6.16$
5	6869	6678	222	13694	f = 0.6

We calculated the tensional and deformational status using the COSMOS/M program, version 2.0.

Having numerous functions and facilities, this program permitted an accurate modeling of the real situations and, in the same time, a complete analysis in which graphic post-processing of the results demonstrated the biomechanical behavior of the structures analyzed.

Results

The program we used has numerous options regarding the data output. Taking into consideration the fact that the present study is dealing with a plane tensional status, the results are express under the form of main tensions $\sigma_1$and σ_2 (the program used the values P_1 and P_2). In most areas of the analyzed structures the σ_1 main tensions are positive (of elongation type) and very small while the σ_2 main tensions are negative (of compressive type) and have high absolute values.

Considering the fact that the main stress acting on the component elements of the analyzed prosthesis is of compressive type, the results were expresses by a representation of the σ_2 main tensions field.

The calculated values for the σ_2 main tensions in points from the proximity of the interface areas of the prosthesis were processed using a special program and afterwards the pressure distribution curves on various contact surfaces.

Pictures (a), (b), (c) and (d) from Figure 3 illustrate the models for the structures that were discreeted using finite elements and the load knots of the four situations analyzed. The colors used in the graphic refer to the four materials used for the calculus:

1 – steel;
2 – femoral bone;
3 – hipbone;
4 – polyethylene.

Pictures (c) from Figures 8–11 show the σ_2 tension field resulted from the calculus for the prosthesis components, femoral bone and hipbone, in all four conditions examined.

Pictures (a) from Figures 8–11 illustrate the details concerning the partial distribution of the σ_2 partial

tensions developed in the proximity of contact area in both femoral head and polyethylene cup.

Using the values of these tensions determined with a processing program, we established the distribution curves for the pressure on the contact surface between the femoral head and the polyethylene cup illustrated in pictures (b) Figures 8–11.

Pictures (d) from Figures 8–11 also show partial details regarding σ_2 main tensions developed in the proximity of both polyethylene cup–armor and armor–hipbone contact areas.

Using the same method mentioned above, pictures (e) from Figures 8–11 illustrate the distribution curves for the pressure at the armor–hipbone contact area.

Discussions

From the data obtained we identified, from one case to another, important variations concerning the tension field distribution in the structures analyzed and the variation of the contact pressure. Based on these observations a series of estimates regarding the biomechanical behavior and reliability of the prosthesis can be made.

By analyzing the σ_2 main tension fields presented in figures (c) from Figures 4–7 we were able to determine the maximal and minimal values for these tensions in the femoral head, polyethylene cup and the hipbone (Table 3).

Table 3

Condition	Tension σ_2 [MPa]					
	Femoral head		Polyethylene cup		Hip bone	
	Max.	Min.	Max.	Min.	Max.	Min.
1	17.70	-176.46	1.090	-15.83	0.608	-70.43
2	5.11	-4.60	0.268	-4.37	0.110	-14.76
3	5.09	-88.05	0.097	-9.48	6.080	-31.18
4	0.003	-3.98	0.080	-3.93	0.003	-3.51

After analyzing the data in Table 3 we observed that the highest compressive tensions (σ_2 = -176.46 MPa) are encountered in the case of the monopod support in the frontal plane for the femoral head of the prosthesis. Considering the fact that these tensions are compressive type tensions, they are harmful and do not damage this part of the prosthesis. In the case of the sagital plane, 15° flexion of the limb and monopod support, the compressive tensions in the femoral head are 50% smaller (σ_2 = -15.83 MPa). These data suggest that the main stress in the case of the femoral head of the prosthesis in the frontal plane.

The data in Table 3 also show that the compressive tensions for the polyethylene cup are relatively small, the highest value also being in the frontal plane and monopod support (σ_2 = -15.83 MPa). The same data also suggest that the maximal tensions in the hipbone are encountered in the frontal plane and monopod support (σ_2 = -70.43 MPa). By examining the σ_2 main tensions field in Figure 5 we observe that these tensions are encountered in the proximity of the contact area with the metallic armor of the prosthesis. As we expected, σ_2 compressive tensions are very small in the case of bipedal support for all the structures analyzed.

The analysis of the variation curves for the pressure on the contact surface illustrated in pictures (b) from Figures 8–11 shows that the highest value for the contact pressure between the femoral head and the polyethylene cup are encountered in the frontal plane and monopod support (σ_2 = 20 MPa). In the case of the sagital plane and monopod support the pressure on the same surface is much smaller (p_{max} = 8 MPa). For the other two situations concerning the bipedal support the maximal values for the contact pressure are low (3 MPa and 4 MPa, respectively).

The high value for the contact pressure recorded between the femoral head and the polyethylene cup in the first situation shows that at this level the chances for the surface of the cup deterioration due to the contact stress are high, e process that would eventually lead to the rapid shortening of the prosthesis life time. The pressure variation curves illustrated in pictures (e) from Figures 8–11 show that maximal value for the contact pressure on the contact area between the armor and the hipbone was also recorded in the frontal plane and monopod support (p_{max} = 25 MPa) (picture e from Figure 8). The maximal pressure in the sagital plane, on the same interface, in monopod support, is much smaller (p_{max} = 8 MPa) (picture e from Figure 10). For the same interface and bipedal support, in both planes, the maximal values of the contact pressure are much smaller (4 MPa and 3 MPa, respectively) (pictures e from Figures 9 and 11).

The very high contact pressure recorded at the armor-hipbone interface (p_{max} = 25 MPa) (picture e from Figure 8) show that in this case there is a risk for bone tissue crush in certain areas of the contact surface. In time these destructions can lead to armor detachment from the bone cavity and thus requiring another surgical procedure. The uneven variations seen in some situations expressed by the peaks recorded in the case of the contact pressure distribution (pictures a and b from Figure 8, d and e from Figure 8, or d and e from Figure 10) are the result of the deficiencies in the contact surface alignment. The same phenomenon is also seen in real life, during the walking process when in certain point of the contact surface pressure variations occur, leading contact stress and dramatic shortening of the prosthesis life time. On the other hand, the fact that the contact pressure at the armor–hipbone and metal prosthetic femoral head–polyethylene cup is half the unique pressure between the metal head and acetabular cartilage (in the case of partial prosthesis) makes us sustain the reliability of the bipolar prosthesis. Concerning the disposition and orientation of the different types of lesions and especially the traumatic ones, the acetabular bone structure is of high significance.

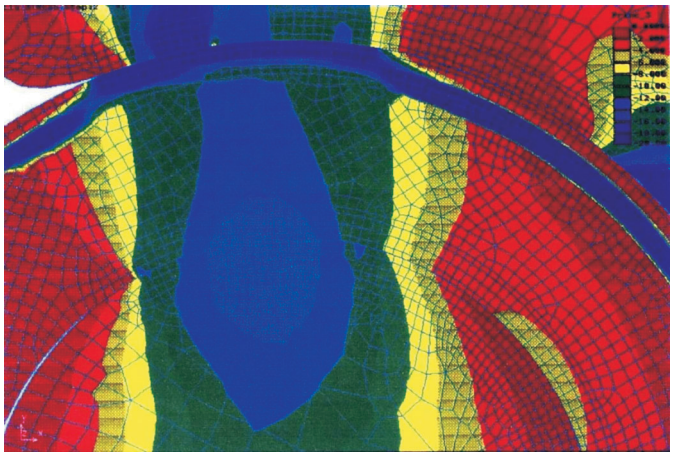

Picture (a) – ***Partial tensions developed in femoral head and polyethylene cup in the proximity of their contact area***

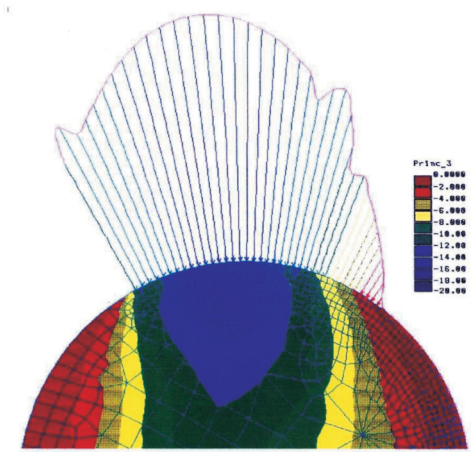

Picture (b) – ***Curves of pressures developed on the femoral head–polyethylene cup contact surface***

Picture (c) – ***General diagram of main tension fields developed in the femoral head, the polyethylene cup and the hipbone***

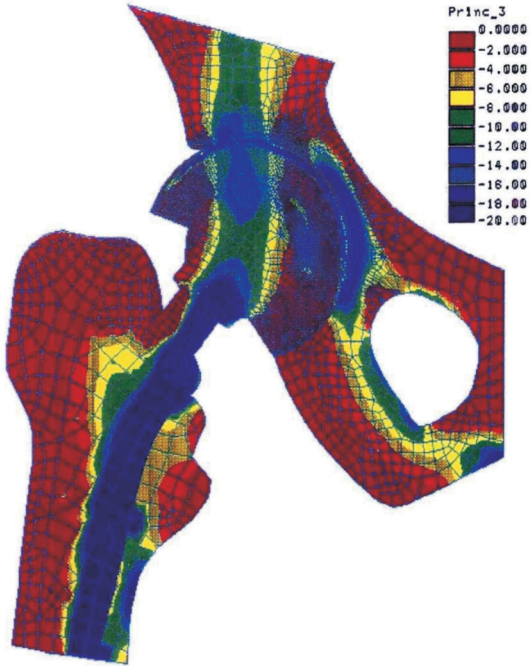

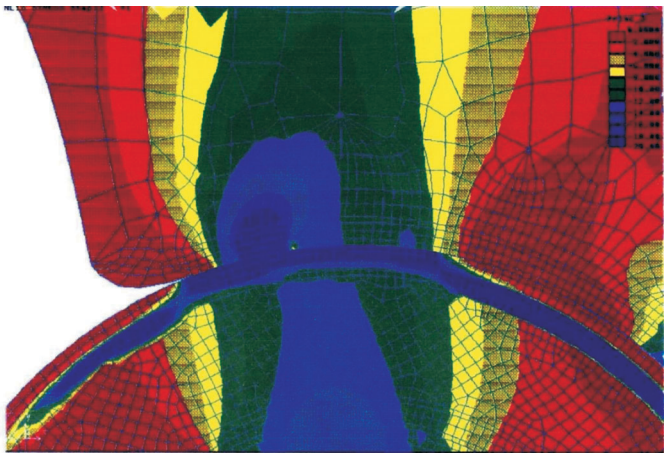

Picture (d) – ***Tensions developed in the proximity of both polyethylene cup–armor and armor–hipbone contact areas***

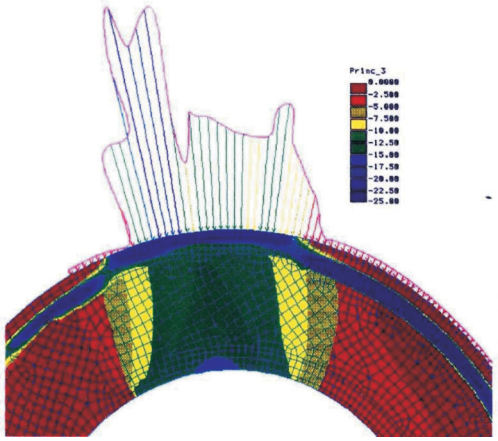

Picture (e) – ***Curves of pressures developed at the armor–hipbone contact area***

Figure 8 – ***Tension and deformation status in condition 1 – frontal section and monopod support***

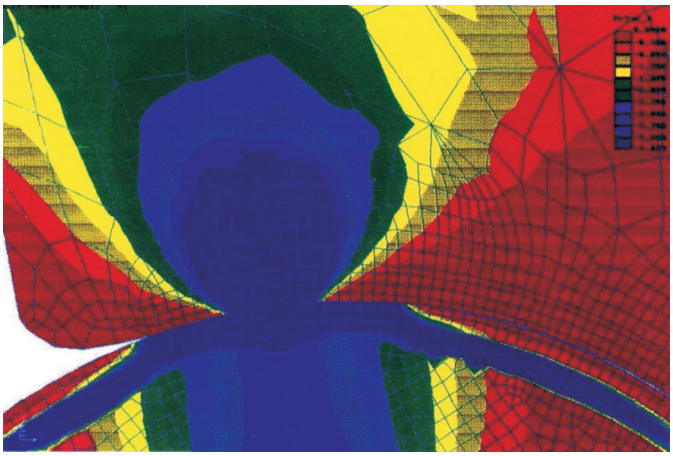

Picture (a) – ***Partial tensions developed in femoral head and polyethylene cup in the proximity of their contact area***

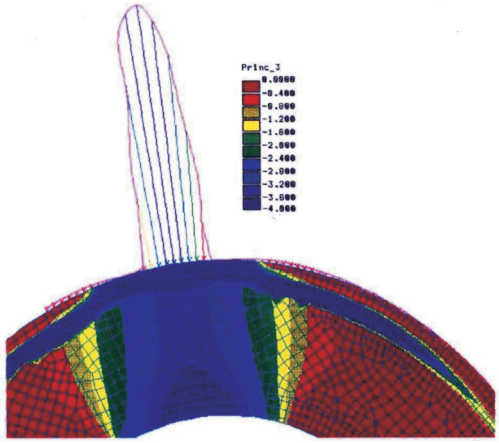

Picture (b) – ***Curves of pressures developed on the femoral headpolyethylene cup contact surface***

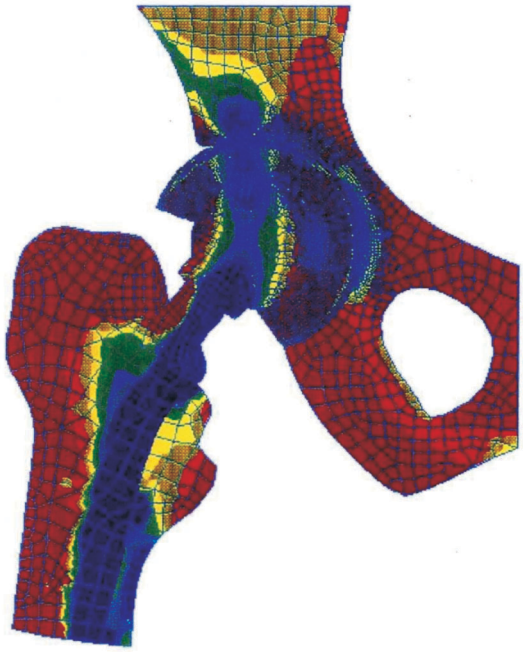

Picture (c) – ***General diagram of main tension fields developed in the femoral head, the polyethylene cup and the hipbone***

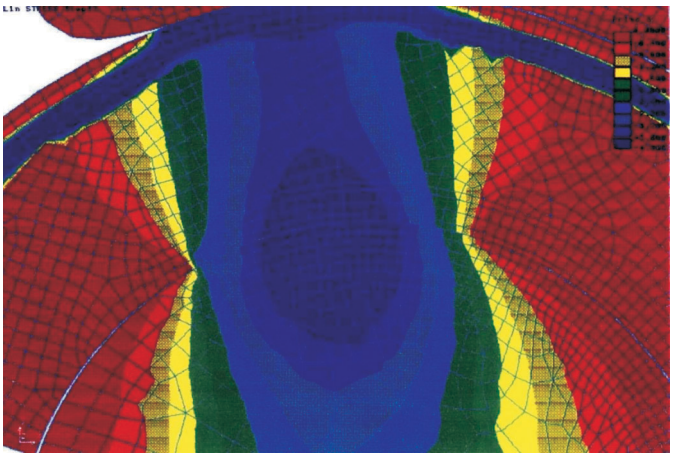

Picture (d) – ***Tensions developed in the proximity of both polyethylene cup–armor and armor–hipbone contact areas***

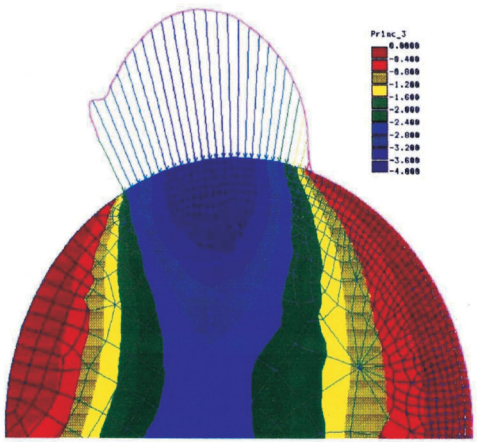

Picture (e) – ***Curves of pressures developed at the armor–hipbone contact area***

Figure 9 – ***Tension and deformation status in condition 2 – frontal section and bipedal support***

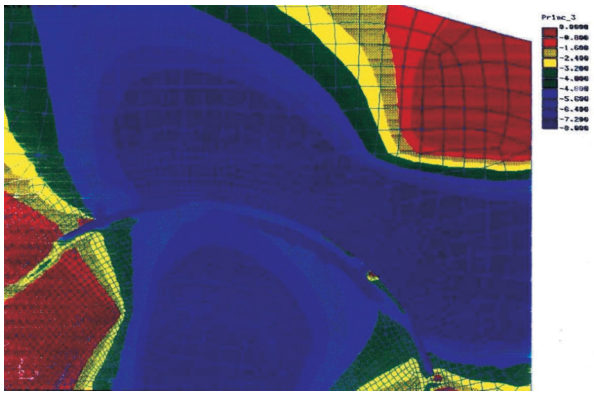

Picture (a) – ***Partial tensions developed in femoral head and polyethylene cup in the proximity of their contact area***

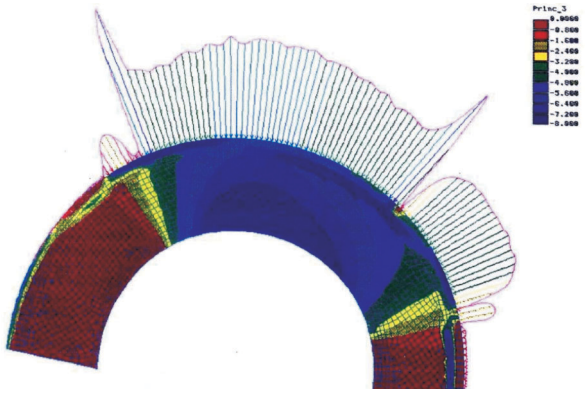

Picture (b) – ***Curves of pressures developed on the femoral head–polyethylene cup contact surface***

Picture (c) – ***General diagram of main tension fields developed in the femoral head, the polyethylene cup and the hipbone***

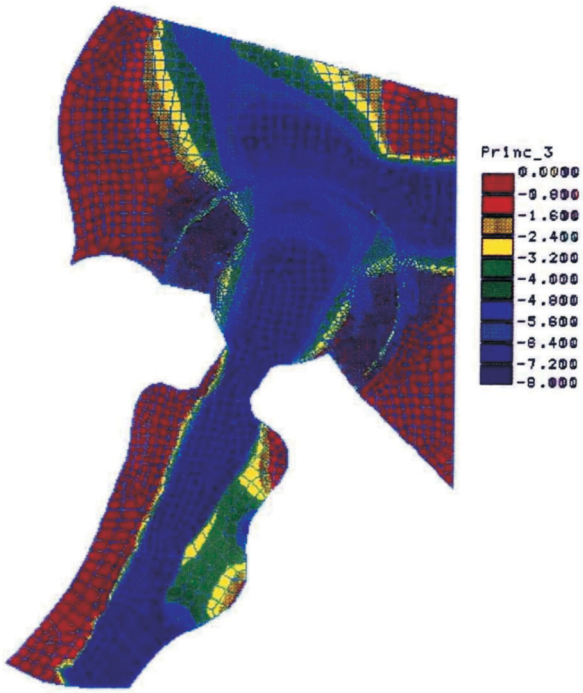

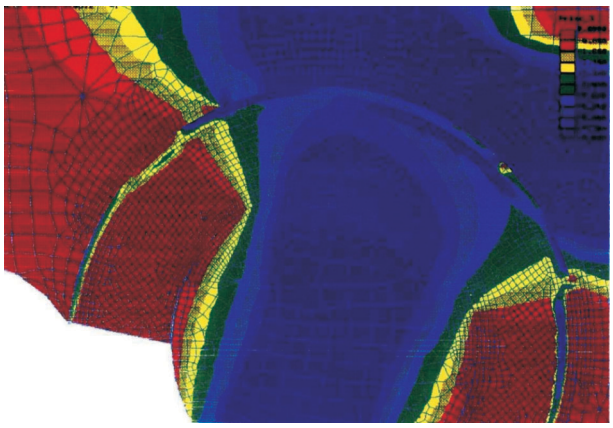

Picture (d) – ***Tensions developed in the proximity of both polyethylene cup–armor and armor–hipbone contact areas***

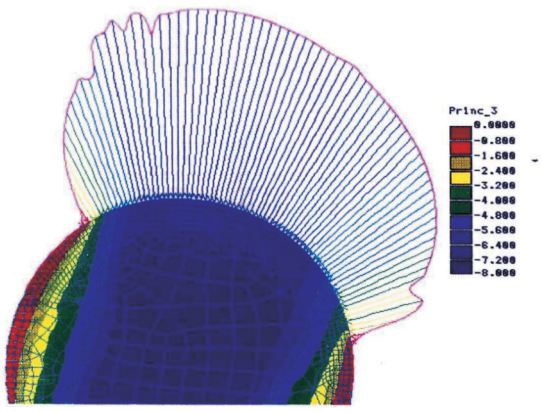

Picture (e) – ***Curves of pressures developed at the armor–hipbone contact area***

Figure 10 – ***Tension and deformation status in condition 3 – sagital section, 15^0 flexion and monopod support***

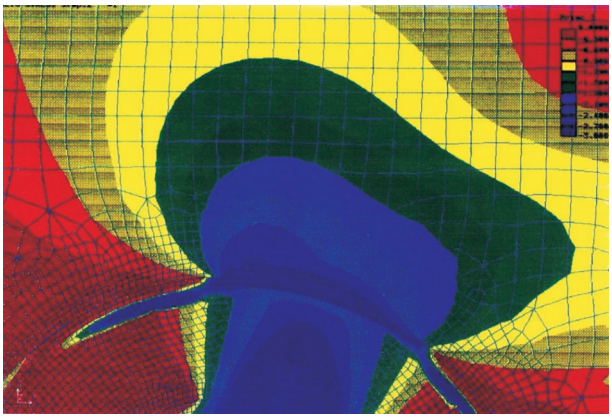

Picture (a) – ***Partial tensions developed in femoral head and polyethylene cup in the proximity of their contact area***

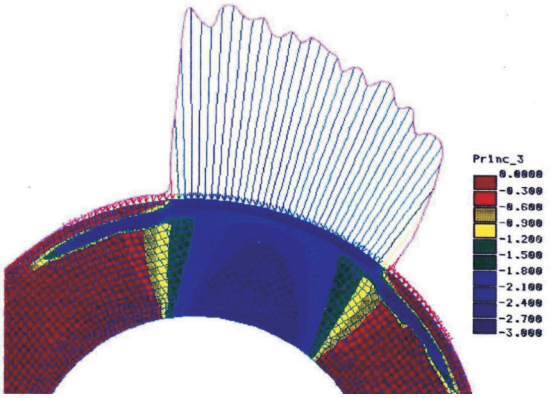

Picture (b) – ***Curves of pressures developed on the femoral head–polyethylene cup contact surface***

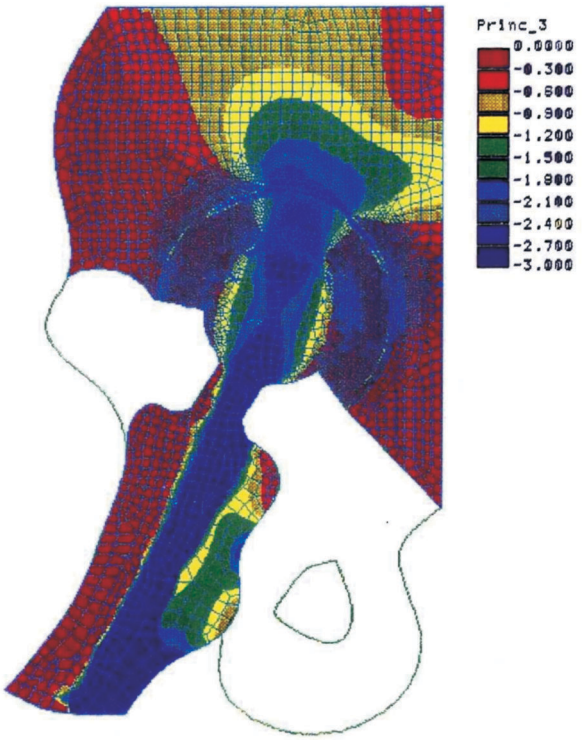

Picture (c) – ***General diagram of main tension fields developed in the femoral head, the polyethylene cup and the hipbone***

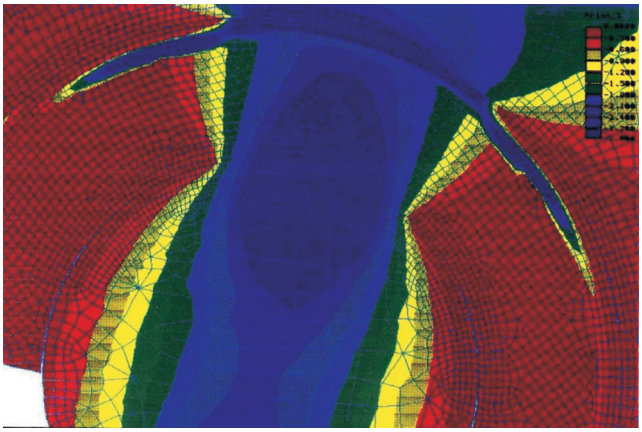

Picture (d) – ***Tensions developed in the proximity of both polyethylene cup–armor and armor–hipbone contact areas***

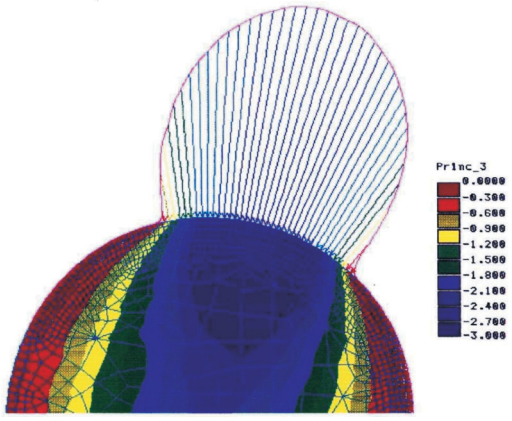

Picture (e) – ***Curves of pressures developed at the armor–hipbone contact area***

Figure 11 – ***Tension and deformation status in condition 4 – sagital section, 15^0 flexion and bipedal support***

Conclusions

The acetabulum and especially the acetabular rim, represent the sight of bone degeneration that accompanies the aging process. One of the most important factors influencing the onset of this morphological deterioration is represented by the mechanic pressure shocks at the contact area between the femoral head and acetabulum with a higher pressure stress on the acetabular rim.

Because of the movement decomposing by the two articulation of the duo cup, and therefore the reduction of the tension and deformation forces that lead to acetabular wear, the bipolar hip prosthesis led to the conservation of the bone capital and a longer period of time without a total prosthesis. Even though, the wear and tear phenomenon is still present.

The histopathological study of the acetabular bone tissue from the surgically removed specimens originating from the same area indicated by FEM will probably identify a series of factors that might reduce the wear and tear phenomenon, and thus delaying the necessity of a total hip prosthesis and the conservation of the bone capital.

Acknowledgements

This work was supported from the Research Project GR50/2006, financed by the Romanian Ministry of Education and Research through CNCSIS.

References

[1] PETERSEN W., PETERSEN F., TILLMANN B., *Structure and vascularization of the acetabular labrum with regard to the pathogenesis and healing of labral lesions*, Arch Orthop Trauma Surg, 2003, 123(6):283–288.

[2] BECK M., LEUNIG M., PARVIZI J. *et al.*, *Anterior femoroacetabular impingement. Part II. Midterm results of surgical treatment*, Clin Orthop, 2004, 418:67–73.

[3] LEUNIG M., BECK M., WOO A. *et al.*, *Acetabular rim degeneration: a constant finding in the aged hip*, Clin Orthop, 2003, 413:201–207.

[4] ANTONESCU D., BUGA M., CONSTANTINESCU I., ILIESCU N., *Metode de calcul şi tehnici experimentale de analiză a tensiunilor în biomecanică*, Ed. Tehnică, Bucureşti, 1986.

[5] BACIU C. C., *Anatomia funcțională şi biomecanica aparatului locomotor*, Ed. Sport–Turism, Bucureşti, 1977.

[6] BLAIMONT P., *Étude biomécanique du femur humain*, Acta Orthop Belgica, 1968, 34(5):670–684.

[7] BLAIMONT P., HALLEUX P., JEDWAB J., *Distribution des contraintes osseuses dans le femur*, Rev Chir Orthop, 1968, 54(4):303–319.

[8] BLAIMONT P., HALLEUX P., *Un paradoxe des contraintes osseuses – rôle du remaniement haversien dans l'adaptation de l'os à sa fonction de soutien*, Acta Orthop Belgica, 1972, 38(1):63–67.

[9] DENISCHI A., ANTONESCU D., ILIESCU N., *Biomecanica*, Ed. Academiei Române, Bucureşti, 1987.

[10] DENISCHI A., DINULESCU I., EŞEANU I. *et al.*, *Cercetări prin tensiometrie în artroplastiile de şold. Biomecanica*, Ed. Academiei Române, Bucuresti, 1989, 166–168.

[11] DUJARDIN F., THOMINE J. M., MOLLARD R., *Étude de la corelation entre la microdureté et la transparence aux rayons "X" de l'extrémité superieure du femur humain*, Rev Chir Orthop, 1991, 77(7):453–461.

[12] BOUSQUET G., GRAMMONT P., *Étude experimentale de la longévité des prothèses de hanche du point de vue mecanique*, Acta Orthop Belgica, 1972, 38(1):123–143.

[13] COMTET J. J., RHUMELART C., BOIVIN M. *et al.*, *Étude de la repartitions des contraintes dans les cupules de prothèses totales*, Acta Orthop Belgica, 1972, 38(1):119–124.

[14] FONTES D., BENOIT J., LORTAT-JACOB A., DIDNY R., *La luxation des prothèses totales de hanche – modélisation mathématique. Approche Biomécanique*, Rev Chir Orthop, 1991, 77(3):151–162.

[15] MEDREA O., BUGA M., ANTONESCU D. *et al.*, *Metode de calcul şi cercetări experimentale în analiza stărilor de tensiune din extremitatea superioară a femurului. Biomecanica*, Ed. Academiei Române, Bucureşti, 1989, 165–169.

[16] PAUWELS F., *Biomécanique de l'appareil moteur*, Springer Verlag, Berlin, 1979.

Mailing address

Dan Anuşca, Associate Professor, MD, PhD, Department of Orthopaedics, University of Medicine and Pharmacy of Craiova, 2–4 Petru Rareş Street, 200 349 Craiova, Romania; Phone +40251–306 110, E-mail: emp@umfcv.ro, pathology@umfcv.ro

Received: September 15th, 2006

Accepted: October 25th, 2006